Supporting Information / Chemistry of Materials

Preparation of Tough Double- and Triple-Network Supermacroporous Hydrogels through Repeated Cryogelation

*Tomáš Sedlačík, Takayuki Nonoyama, Honglei Guo, Ryuji Kiyama, Tasuku Nakajima, Yoshihiro Takeda, Takayuki Kurokawa, Jian Ping Gong**

Table of Contents:

Characterization of SN cryogels in detail

SN cryogels were coded as M_1-x_1, where M_1 is the total monomer concentration (mol L^{-1}) including the crosslinker and x_1 is the molar ratio of crosslinker MBAAm relative to the monomer NaAMPS (mol%) in the solution of gel precursors. The appearance of the SN cryogels based on PNaAMPS varied from transparent to opaque depending on the amount of the crosslinker used for the preparation (1 mol.% transparent, 4 mol.% semi-transparent, 8 mol.% nearly opaque). As an example, the visual appearance of SN cryogel 0.44-4 and its cross-sectional morphology, as revealed by SEM, are shown in **Figure S1a, b.** The morphology of other SN cryogels is presented in **Figure S2**. All the prepared SN cryogels showed the structure with interconnected pores of a similar size (~ 50–100 μm in diameter), which is determined mainly by the freezing temperature, geometry of samples, and swelling of the sample after preparation. The effect of the freezing temperature on the pore size of cryogels is well known. Cryogels with smaller pores are formed at lower temperatures and *vice versa*. In this study, we kept the cooling temperature constant for all samples (-16 °C), that resulted in pore sizes suitable for accommodating various cells. Note that solutions with high monomer concentration and crosslinker ratio tended to form a less porous or non-porous skin layer on the cryogel surface (see also Figure S2). Samples with a composition with a strong tendency to form this type of skin layer were not used for subsequent preparation of DN cryogels. The relative volumetric change, equilibrium water regain (water in macropores and gel phase together), and porosity (determined by cyclohexane uptake and as described in methods) of the SN cryogels are shown in **Figure S1c, d.** For example, SN cryogel 0.44-4 increased its volume by factor *Qv* = 4.6, contained a high amount of water per dry polymer: 40.6 g/g and its macropores occupied 96.5%.

The mechanical properties of the SN cryogels were evaluated under compression, as all these samples were brittle. However, the SN cryogels possessed a relatively broad range of

mechanical properties, with compressive modulus ranging from ~3 kPa to ~350 kPa (**Figure S1e, f**). A higher concentration of monomer solution or crosslinker ratio resulted in a higher modulus of the resulting cryogel. However, the more rigid gels were more brittle and showed either bulk fracture (samples 0.44-8 and 0.88-8) or irreversible damage when compressed to a large strain (sample 0.88-4). According to DN theory, the introduction of the ductile 2nd network could, therefore, lead to significantly tougher cryogels.

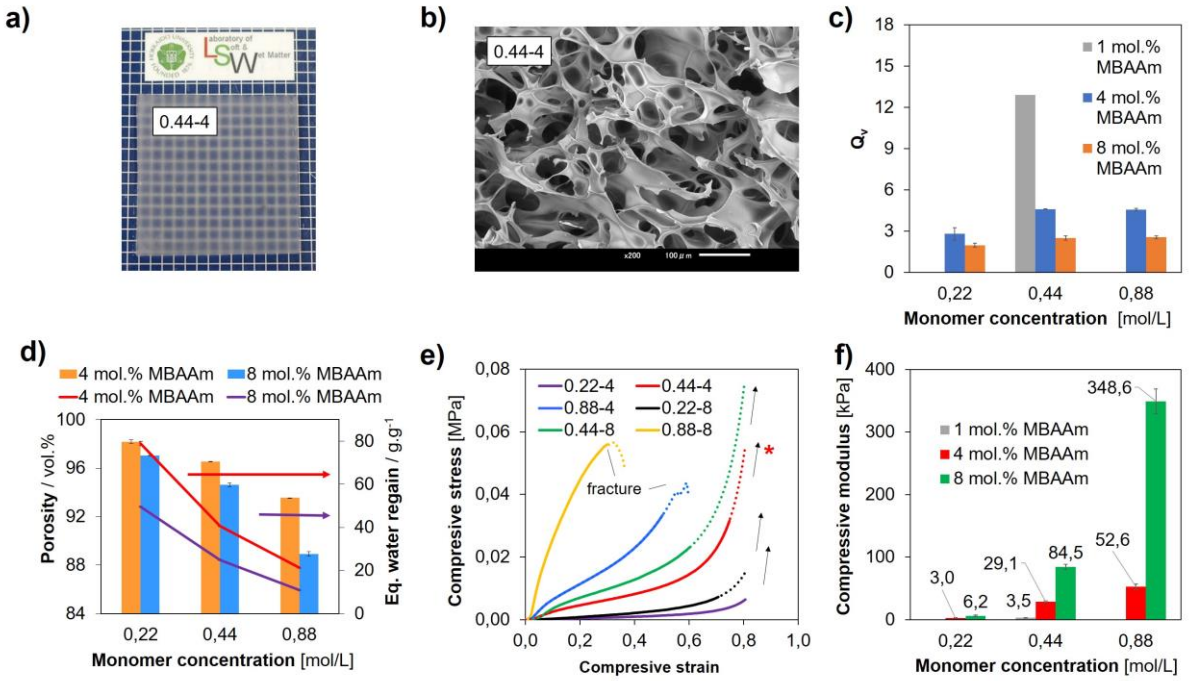

Figure S1. Properties of PNaAMPS SN cryogels prepared from monomer solutions with various formulations (M_1-x_1). The visual appearance of SN cryogel 0.44-4 **(a)**. Morphology of interconnected macropores was observed for all prepared cryogels; SN cryogel 0.44-4 is shown as a typical example, the scale bar is 100 µm **(b)**. The relative volumetric change *Qv* of SN cryogels by swelling relative to the as-prepared state **(c)**; dependence of porosity and equilibrium water regain **(d)**, compressive stress-strain curves **(e)**, and compressive modulus **(f)** of SN cryogels. The average values and the corresponding standard deviations were determined for at least three samples; for the compressive test (e), the cryogels were compressed up to 80% or until macroscopical fracture (dashed lines), and the solid lines represent compressibility of cryogels without evidence of any internal damage (almost no irreversible deformation).

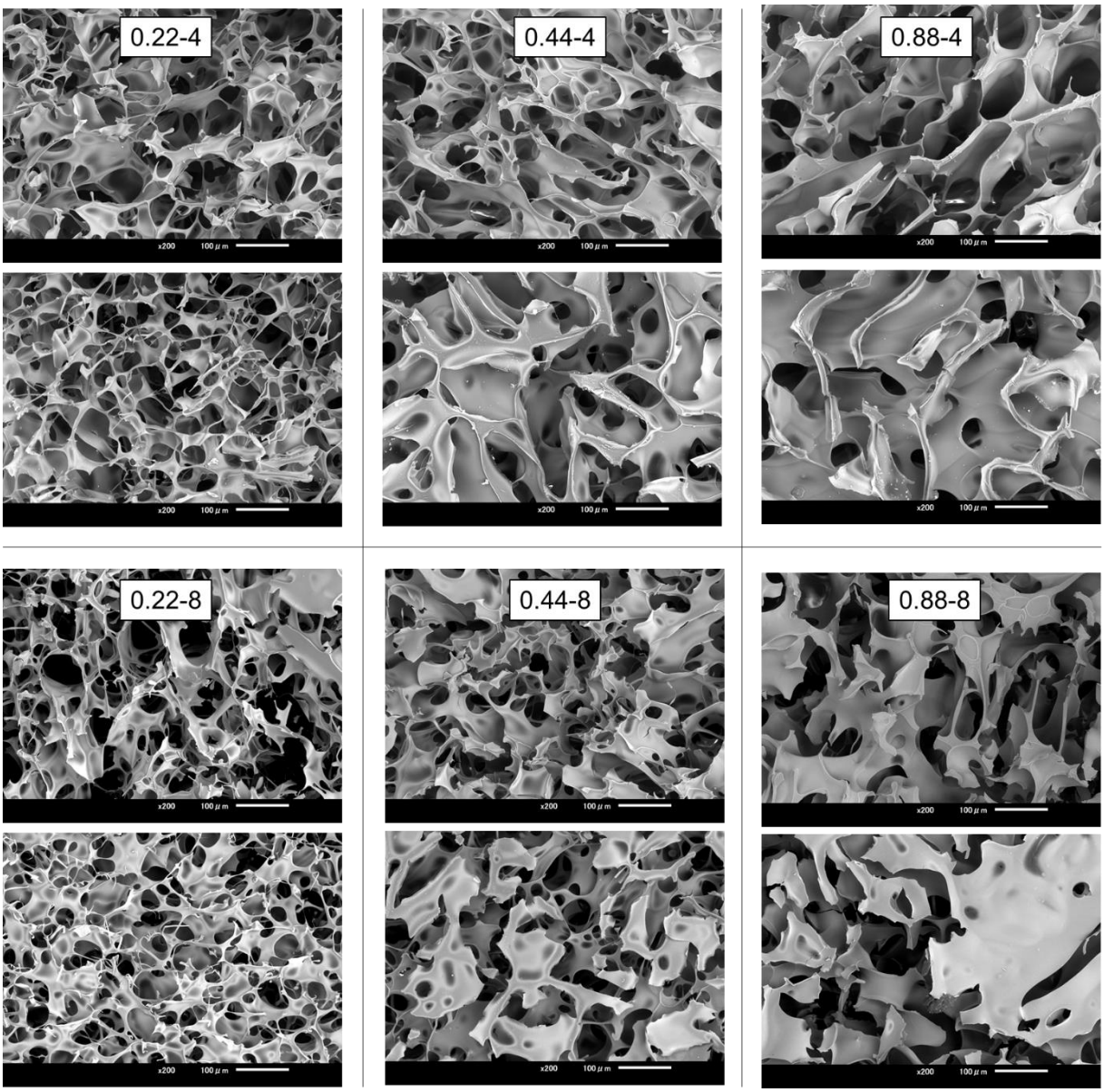

Figure S2. Morphology of PNaAMPS SN cryogels visualized by SEM. The coding represents the gel composition (M_1-x_1). The scale bar is 100 μm. All cryogels had a similar architecture of interconnected macropores. The upper pictures represent the cross-sectional morphology, while the lower pictures represent the corresponding surface views. The samples prepared from solutions with a high monomer concentration and crosslinker ratio tended to form a less porous or non-porous skin layer on the surface.

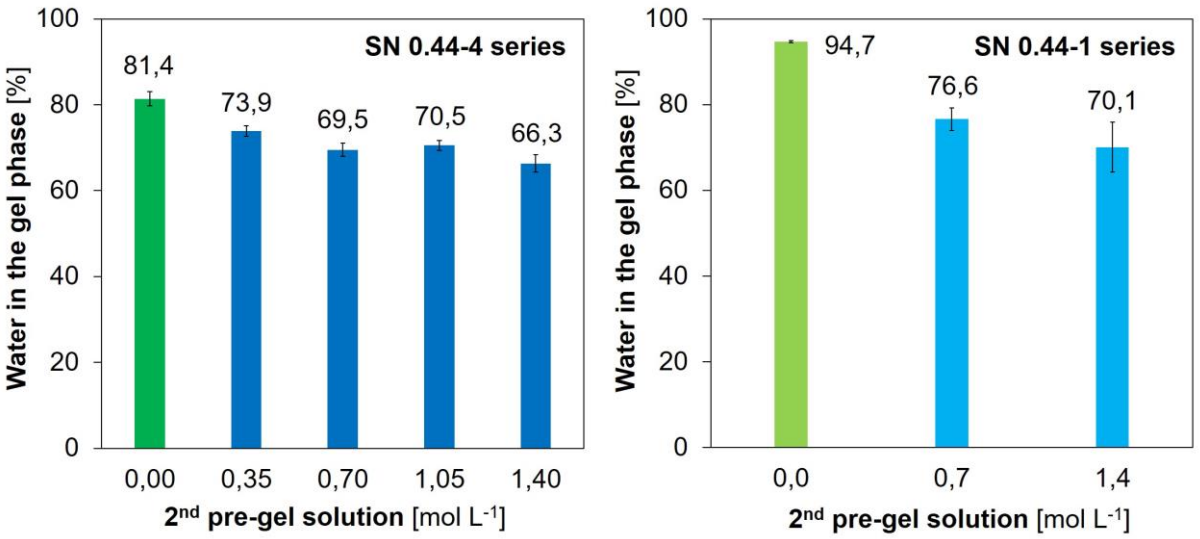

Figure S3. Water in the gel phase of DN cryogels determined by the gel squeezing experiment ($W_{\%GEL}$ as described in Experimental section). DN cryogel series made of SN cryogel 0.44-4 **(left)** and SN cryogels 0.44-1 **(right)**. 2nd pre-gel solution concentration 0.0 mol L^{-1} represents respective SN cryogels (in green).

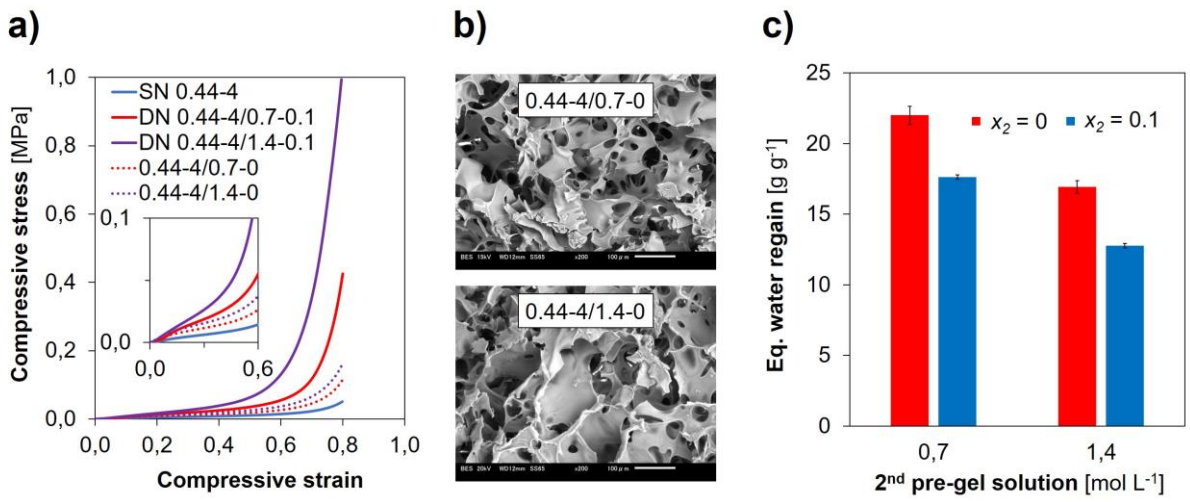

Figure S4. Comparison of the mechanical properties of DN cryogels prepared from SN cryogel 0.44-4 with their corresponding semi-IPN cryogels (a). The equilibrium water regain of semi-IPN cryogels and their corresponding DN cryogels (b) and morphology of semi-IPN cryogels visualized by SEM (c). The 2nd network in DN cryogels was sparsely crosslinked (x_2 = 0.1 mol.% of MBAAm), while there was no crosslinker in semi-IPN cryogels (x_2 = 0). Despite an improvement in the mechanical properties of semi-IPN cryogels when compared to the original SN cryogel, DN cryogels clearly showed significantly higher toughness. Semi-IPN cryogels contained slightly more water than DN cryogels and, as expected, showed a similar morphology of interconnected macropores (compare Figure S4b and Figure 2c). The scale bar is 100 µm.

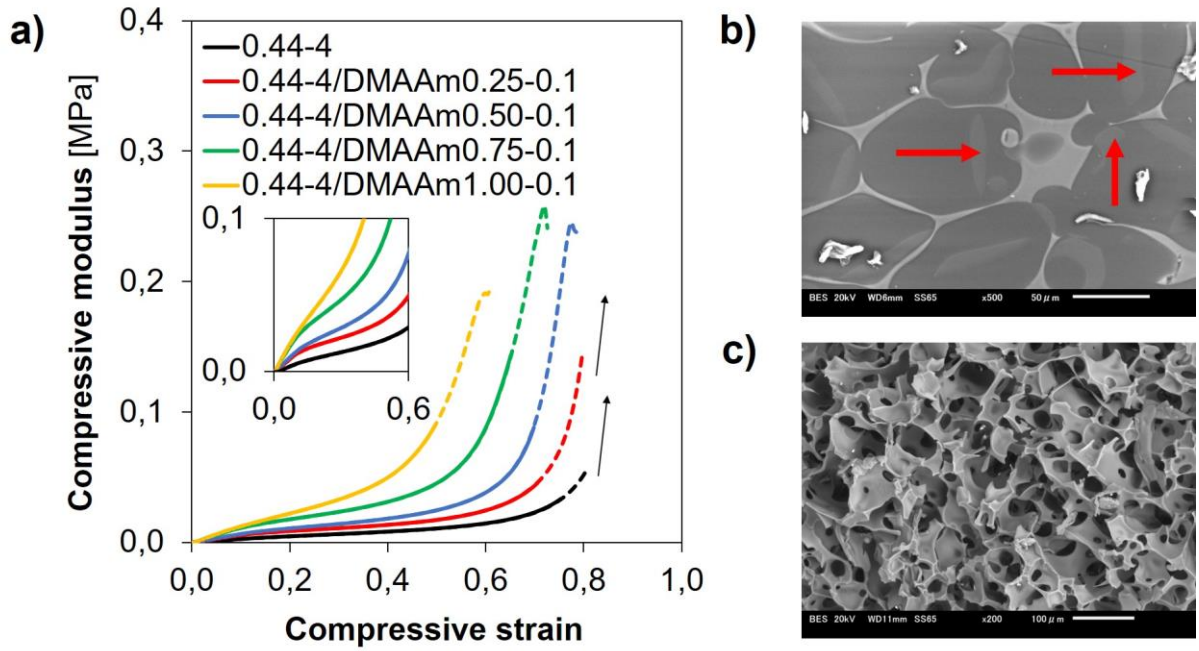

Figure S5. Compressive test of DN cryogels made from PNaAMPS/PDMAAm (a), the structure of cryogel 0.44-4/DMAAm0.5-0.1 fixed in resin (b) and freeze-dried (c), visualized by SEM. For the compressive test, the cryogels were compressed up to 80% or until macroscopical fracture (dashed lines), and the solid lines represent compressibility of cryogels without evidence of any internal damage (almost no irreversible deformation). In (b), since the BSE detector was used, the PNaAMPS/PDMAAm DN region, which contained sulfur and was more crosslinked and denser, appears as the brighter phase, while PDMAAm phase appears as the less bright phase (indicated by arrows). The scale bar is 50 µm in (b) and 100 µm in (c).